Phase Transitions of Malonic and Oxalic Acid Aerosols

Christine F. Braban,* Matthew F. Carroll, Sarah A. Styler, and Jonathan P. D. Abbatt*

Department of Chemistry, University of Toronto, 80 St. George Street, Toronto, Ontario M5S 3H6, Canada

Received: February 25, 2003; In Final Form: May 1, 2003

Atmospheric aerosol has been shown to contain an organic component that includes a significant fraction of small dicarboxylic acids, particularly in the urban environment. As an initial step toward understanding the phase in which particles may exist, a detailed study into the phase transitions of malonic and oxalic acid aerosols has been carried out. Both the aerosol phase transitions (deliquescence and efflorescence) and bulk solution properties (equilibrium water vapor pressure and the solubility and freezing curves of the aqueous solutions) are reported. An aerosol flow tube-FTIR and a static mode chamber-FTIR have been used to identify particulate phase transitions. In the latter the particles can be observed under ice-supersaturated conditions, allowing investigation of behavior at subeutectic temperatures. We report that both malonic and oxalic acid aerosols sustain a substantial level of solute supersaturation before efflorescence occurs, whereas deliquescence occurs at the thermodynamically predicted relative humidity. At room temperature, malonic acid efflorescence is observed at RH = 6% ± 3% and oxalic acid efflorescence occurs at RH ≤ 5%. Malonic acid particles deliquesce between 69% and 91% RH over the temperature range 293−252 K, and for oxalic acid conditions close to 100% RH are required. We report the first observation of the phase transition of oxalic acid between the anhydrous and dihydrate form and discuss our results in the context of recently published data.

1. Introduction

Low molecular weight dicarboxylic acids are ubiquitous and abundant water-soluble organic species in tropospheric aerosol. It is therefore important to understand the effects these acids may have on the phase and chemical properties of aerosols that have been traditionally considered as inorganic salts. In this paper we consider two of the smaller water-soluble organic acids: malonic acid and oxalic acid. Oxalic acid (HOOCCOOH) is present in both the gas phase and the aerosol phase and frequently has the highest concentration of all the identified dicarboxylic acids in the condensed phase, followed by malonic acid ($HOOCCH_2COOH$). The bulk physical properties of oxalic acid and malonic acid are not presented here but can be found in some recent studies.[1−3]

The sources of dicarboxylic acids in the atmosphere are disparate and include primary anthropogenic, and secondary anthropogenic and biogenic, specifically degradation products from larger organics. Several field campaigns have analyzed Arctic aerosols for dicarboxylic acids, with typical values those of Narukawa et al.,[4] who reported oxalic acid and malonic acid present at 21.8 and 4.14 ng·m^{-3}, respectively. Yao et al.[5] observed, in urban aerosol, levels of oxalate to be on average 370 ng·m^{-3} and levels of malonate 90 ng·m^{-3}. The range 0.18−1.14 μg·m^{-3} has been reported for concentrations of oxalic acid in urban aerosol.[6,7] The sum of the dicarboxylic acid concentrations (in micrograms per cubic meter) can constitute 4−7% of the sulfate concentration[5] and some studies indicate that in polluted urban environments the concentrations of organic acids can be high enough to make effective cloud condensation nuclei.[8]

The focus of this work is to investigate the phase of organic acid particles. Particle phase affects both the direct and indirect effects of aerosols on climate, and so a thorough understanding of aerosol phase transitions under atmospheric conditions is needed. In particular, it is important to understand in detail simple binary organic−H_2O systems before complex mixed inorganic−organic systems are considered. One of the phase transitions of interest is deliquescence, the uptake of water by a dry solid to form an aqueous solution. The reverse process, i.e., the loss of water to form a dry crystalline solid, is called efflorescence. Various techniques have been used to investigate deliquescence and efflorescence of inorganic particles including aerosol flow tube Fourier transform infrared spectroscopy (AFT-FTIR),[9−12] optical microscopy,[13] and electrodynamic balance studies.[14,15] The process is generally characterized by the relative humidity of the phase transition as a function of temperature. Relative humidity (RH) is reported throughout this study, as it is useful to interpret the composition-temperature phase diagram and is an atmospherically relevant quantity. At a specific temperature (T), the RH is calculated from the measured water partial pressure, $p(T)$:

$$\mathrm{RH} = 100\frac{p(T)}{p^{\mathrm{sat}}(T)}$$

where $p^{\mathrm{sat}}(T)$ = saturated vapor pressure of pure water at temperature T.

In general, at temperatures above the eutectic, deliquescence of inorganic salts occurs at the thermodynamic equilibrium deliquescence RH (DRH) and recent studies indicate that a similar transition to metastable deliquesced particles can also occur below the eutectic temperature.[13,15−17] Efflorescence in inorganic aerosols occurs at a substantive level of solute supersaturation and there is variability between chemical species as to whether they exhibit homogeneous efflorescence under atmospherically relevant conditions. For instance, micrometer-sized ammonium sulfate particles effloresce homogeneously between 35% and 40% RH, whereas ammonium bisulfate particles do not effloresce under most experimental conditions.

* Corresponding authors. E-mail: cbraban@chem.utoronto.ca. E-mail: jabbatt@chem.utoronto.ca.

10.1021/jp034483f CCC: $25.00
Published on Web 08/07/2003

In this paper we present a suite of atmospherically motivated experiments involving oxalic acid and malonic acid aqueous solutions. Specifically we have carried out (i) bulk solution studies of the ice-solution and crystalline salt-solution coexistence curves; (ii) equilibrium water vapor pressure measurements of these systems; and (iii) deliquescence and efflorescence experiments in an aerosol flow tube system (AFT) and also in a static mode chamber system (SMC), with aerosol particles supported on a silicon surface. Experiments characterizing malonic acid aerosol deliquescence are presented both above and below the eutectic temperature. The oxalic acid−water system proved more complex than the simple binary eutectic, and therefore only supraeutectic deliquescence observations were possible. A few recent studies have focused on phase transitions of dicarboxylic acid particles both as the pure acid in aqueous solution and in ternary solution with an inorganic component.[1,2,18,19] These will be discussed in the context of the results from this study in Section 4.

2. Experimental Section

2.1. Bulk Solution Measurements. Equilibrium solution composition and water vapor pressure experiments were performed with both malonic and oxalic acid to correlate relative humidity to solute concentrations in aerosol experiments. Water vapor pressures were measured as a function of temperature. Also, the equilibrium temperatures of ice-solution and acid-saturated solution conditions were investigated for a range of solute concentrations. All solutions were made from reagent-grade chemicals and 18 MΩ water. Malonic acid was from Sigma Chemical Co. (99% purity) and oxalic acid was purchased as oxalic acid dihydrate from Fisher Scientific (assay: 99.86%). Control experiments for pure water were also performed by the methods below.

Water vapor pressure measurements were carried out in a small sealed glass vessel in which the pressure was monitored by a manometer (MKS 622A, full scale 100 Torr). A small volume of acid solution (usually 10 mL) was placed in the vessel and degassed via freeze−pump−thaw cycles. The vessel was then placed in a temperature-controlled circulator bath (Fisher Scientific Isotemp 1006S) and allowed to equilibrate for 1 h. Pressure was recorded as a function of time, and after equilibration, the temperature was increased and the system was allowed to reequilibrate. Malonic acid experiments were performed between 274 and 293 K, and oxalic acid experiments between 288 and 318 K. The leak-up rate for the apparatus was measured regularly, both with and without sample in the vessel. The leak-up rate was found to be between 0.06 and 0.21 mTorr·min^{-1} and was subtracted from the measured pressure as a function of time. After completion of vapor pressure measurements for a solution, a 2.5 mL aliquot of the solution was sampled and diluted to 100 mL. The diluted solution was titrated with 0.500 M NaOH solution and the derivative of the titration curve used to obtain the acid-equivalence points, the second of which was used to calculate the concentration of the acid solution. Error in the concentration measurements has been calculated to be ±1%.

To investigate the solid−liquid coexistence curves, it is necessary to sample a solution under conditions at which both solid and liquid phases are present at equilibrium. An aliquot (10 mL) of solution was placed in the glass vessel and vacuum was applied for several seconds. This measure provided protection against overpressuring for experiments to be carried out at higher temperatures. The solution was taken to a temperature at which no solid phases were present and then cooled until a significant amount of solid matter was observed. The temperature was then adjusted to that of interest and the system was allowed to equilibrate for approximately 3 h, at which point 1 mL of solution was sampled. Sampling at intervals up to 6 h of equilibration time were carried out in two experiments to confirm that equilibrium had been reached in the 3 h experiments, which was the case. The concentration of acid in the sampled solution was determined by titration as described above.

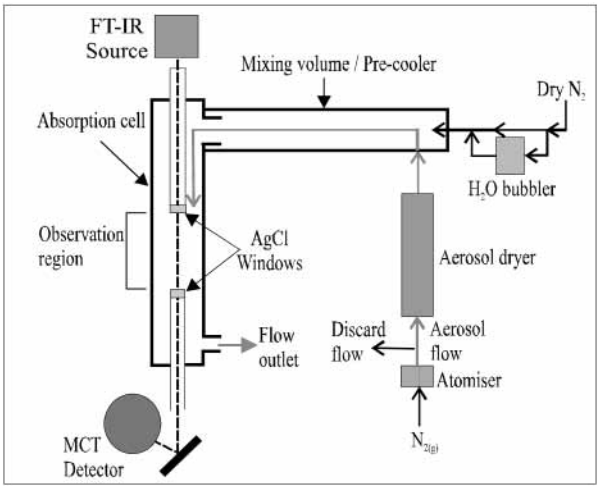

Figure 1. Schematic of aerosol flow tube−Fourier transform infrared spectrometer apparatus.

2.2. AFT Experiments. The AFT-FTIR spectrometer system (hereafter referred to as AFT) is shown schematically in Figure 1. This apparatus has been previously described.[9,20,21] Experiments are carried out by incrementally adjusting the RH. Increasing the RH is termed deliquescence mode, and decreasing the RH is termed efflorescence mode.

Aerosol is produced with a commercial atomizer (TSI model 3076), and a fraction of the aerosol flow is discarded while the remainder either passes through a silica gel dryer (TSI 3062) or bypasses the dryer for the deliquescence and efflorescence experimental modes, respectively. The aerosol flow is mixed with a 2 L·min^{-1} nitrogen flow, a fraction of which can be saturated with water vapor by passage through a water bubbler assembly.

The total flow (between 2.3 and 3.0 L·min^{-1}) then passes through a precooler-mixing volume before entering the main aerosol flow tube. The residence time of the aerosol in the flow tube is between 0.2 and 0.3 min depending on the flow rates of the particular experiment. Both the flow tube and the precooler-mixing volume are temperature-jacketed with the temperature controlled by use of a circulator (Julabo FP88-MW). The temperature in the flow tube is measured with two T-type thermocouples. The thermal gradient over the observation region is less than 0.2 K in all the experiments performed and is generally less than 0.1 K.

A length of 40 cm in the flow tube is monitored with the FTIR spectrometer (Bomem MB104). IR spectra are recorded over the wavenumber range 4000−500 cm^{-1} with a resolution of 4 cm^{-1}. The RH in the flow tube is measured via a gas-phase water line calibration, integrating the area under 1710−1690 cm^{-1}. The calibration was carried out in two ways: (i) by mixing of known flows of dry and saturated N_2 at constant temperature and (ii) by calibration under ice-saturated conditions between 213 and 270 K. An example calibration curve from method (i) is shown in Figure 2. The points are fitted by a fourth-order polynomial fit, and interpolated values from this curve are used as the water-line calibration. All calibrations are

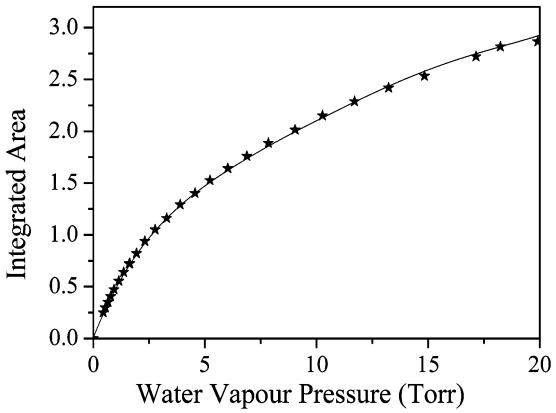

Figure 2. Gas-phase water-line calibration: Integration of area 1410−1390 cm^{-1}.

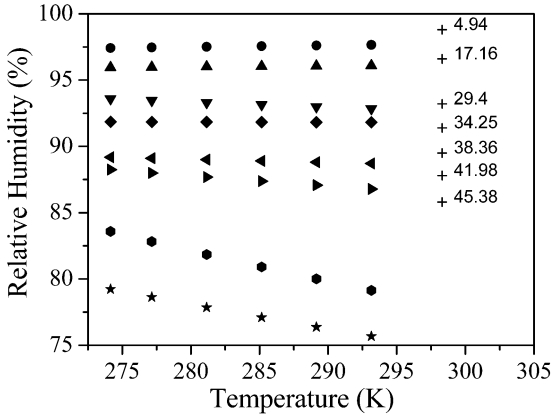

Figure 3. Equilibrium relative humidity above malonic acid solutions as a function of temperature. Solution composition key (wt % malonic acid): ●, 5.6; ▲, 15.0; ▼, 28.2; ◆, 32.0; left-facing triangle, 41.1; right-facing triangle, 47.1; ⬣, 53.0; ★, 59.3; +, Peng et al.[2] (compositions as labels).

in agreement to within 3% over the full RH range, and in general the confidence level of reported relative humidities is ±1%. The calibration is checked during each experiment by setting the system to water-saturated conditions.

For deliquescence-mode experiments the system is initially at the lowest RH attainable, i.e., 2 L of dry N_2 added to the "dry" aerosol flow that has passed through the silica dryer. The RH is incrementally increased until close to water-saturated conditions are present in the AFT. Conversely, in an efflorescence-mode experiment a "wet" aerosol flow is initially mixed with a saturated N_2 flow and the RH is incrementally decreased. For each measurement, the system is allowed to stabilize after the RH is adjusted. Then the infrared spectrum is recorded and the RH is then incrementally either increased or decreased depending on the experimental mode. Infrared spectra were recorded as an average of 50 scans at 4 cm^{-1} resolution. From the infrared spectrum, the RH is measured by the gas-phase water-line calibration as described above. The condensed-phase features of the aerosol infrared spectrum are used to determine the phase of the aerosol and the RH at which phase transitions occur. This is ascertained by subtracting from the aerosol spectrum that of aerosol at the lowest RH for that experiment. The resulting spectra are analyzed for condensed-phase water as a function of RH. Also, analyses of "difference spectra" obtained by subtracting infrared spectra at subsequent relative humidities were used to pinpoint the RH of a phase transition.

2.3. SMC Experiments. Deliquescence at subeutectic temperatures takes place under conditions that are supersaturated with respect to ice formation. Braban et al.[16] and Fortin and Tolbert[17] recently presented quantitative measurements of the deliquescence RH of ammonium sulfate (particles and thin films respectively) at temperatures below the eutectic of the ammonium sulfate-water system (254 K). Between 203 and 254 K deliquescence occurred within experimental error of the thermodynamically predicted value. Between 181 and 203 K, Fortin and Tolbert[17] observed both ice deposition and deliquescence processes occurring with equal frequency, and below 181 K, ice deposition was the sole mechanism for formation of condensed-phase water on ammonium sulfate films.

A static mode chamber (SMC) previously described in Braban et al.[16] is used to investigate malonic acid deliquescence below the eutectic temperature, 260 K. To achieve ice-supersaturated conditions, aerosol particles are placed on an optically smooth silicon window that is held in the vacuum chamber. The silicon window is centered in the optical path of a Fourier transform infrared spectrometer (Nicolet Magna 550 Series II) so that the phase and solution characteristics of particles can be monitored. The entire path length of the IR beam was purged with dry, CO_2-free air while outside the chamber.

The silicon window is cooled such that it, and the particles on it, are the coldest part of the system. In a deliquescence experiment, a constant pressure of water vapor is maintained in the chamber and the temperature of the window is lowered. The pressure in the chamber is monitored with two capacitance manometers, with ranges of 0−1 and 0−10 Torr (MKS 220). Pressure variability in an experiment is generally less than $\pm 5 \times 10^{-4}$ Torr, and the total pressure due to air leaks was less than 2×10^{-4} Torr. Two thermocouples calibrated over the temperature range 303−223 K are used to measure the window temperature and to verify that the window is the coldest part of the system. To ensure good thermal contact between the thermocouple and the silicon, the thermocouple tip is mounted under a PTFE washer, held to the surface of the window by a small nut and screw. The temperature gradient across the window was found to be a maximum of 0.3 K at 233 K. The temperature of the particles and the water vapor adjacent to the window are estimated to be very similar given that the gaseous mean free path is much smaller than the chamber dimensions.

Particles used in the malonic acid experiments are generated with an atomizer (TSI 3076). The aerosol flow is applied to the window for approximately 3 min, which leads to a coverage of fine droplets. Infrared spectra are taken over the frequency range 4000−500 cm^{-1} with a resolution of 4 cm^{-1}. Quantitative experiments with oxalic acid were not performed because the vapor pressure of oxalic acid was sufficiently high that under the vacuum conditions used ($<1 \times 10^{-4}$ Torr) the oxalic acid particles evaporated over the time scale of an experiment. A few experiments in which a dropper pipet was used to crudely form a film were performed to qualitatively confirm AFT experimental observations at low relative humidities. The results from these experiments will be discussed briefly in Section 3.3.

3. Results

3.1. Bulk Solution Measurements: Water Vapor Pressures. In Figures 3 and 4 the equilibrium RH of malonic acid and oxalic acid solutions are presented as a function of temperature and composition, respectively. For malonic acid, we have compared our results to Raoult's law for each temperature and find good agreement between the two, with only the most concentrated solutions at the highest temperatures exhibiting a significant negative deviation from ideality. In some

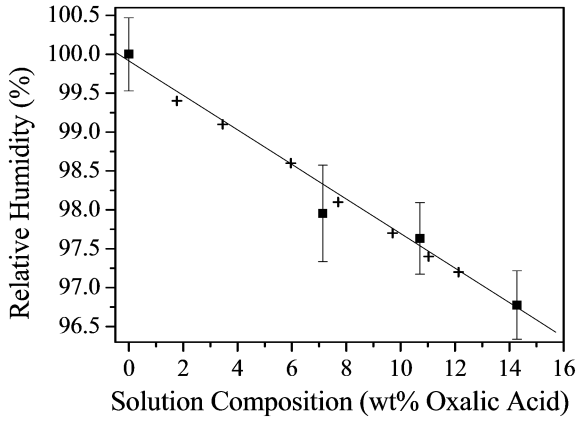

Figure 4. Equilibrium relative humidity above oxalic acid solutions as a function of composition. (■) This work (see Table 1 for temperature ranges used to calculate average RH for each composition); (+) Peng et al.,[2] experiments performed at $T = 298$ K.

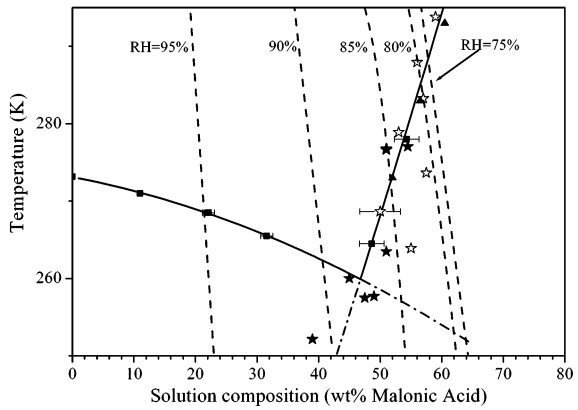

Figure 5. Malonic acid−H_2O binary phase diagram. (—) Ice−$C_3H_4O_{4(aq)}$ (left-hand side) and $C_3H_4O_{4(s)}$–$C_3H_4O_{4(aq)}$ (right-hand side) coexistence curves; (— · —) extrapolation of coexistence curves; (---) constant relative humidity contours; (■) solid−liquid coexistence curve measurements (error bars represent 2 SD); (▲) literature data.[22] Aerosol experiments: (☆) AFT results; (★) SMC results. (Error bar represents 2% RH and is estimated to be approximately the same for both experiments.)

of the measurements the solution was supersaturated with respect to malonic acid; however, no precipitation was observed in those experiments. Selected bulk solution results from the room-temperature study by Peng et al.[2] are also shown in Figure 3. These results agree to within 2% of our values and in most cases the deviations are less than 1%.

By fitting the malonic acid vapor pressure data as a function of composition, RH contours were generated (see Figure 5, Table 1B). The uncertainty associated with these contour lines increases when it is extrapolated beyond the temperature range of the experiments (above 293 K and below 274 K) and also RH ≤ 80%, as there are fewer data points in this region. For RH ≤ 80% the uncertainty is estimated to be ±3%, whereas at RH > 80% the uncertainty is estimated to be ±1%. The latter is supported by the agreement with the data from Peng et al.[2]

Due to the relatively low solubility of oxalic acid (e.g., 11.2 wt % at 297 K; ref 3), the maximum oxalic acid concentration studied was 14.3 wt %. Three solutions were studied over the temperature range 288−318 K. Over this temperature range the RH was found to be constant within the errors of the experiment (see Table 1D).

The equilibrium RH as a function of solution composition is shown in Figure 4. The RH for each composition reported here is the average value over the temperature range studied. Error

TABLE 1: Summary of Experimental Data Used to Construct Relative Humidity Contours and Equations of Solid−Liquid Coexistence Curves for Binary Phase Diagrams[a]

Malonic Acid
(A) Relative Humidity (%)

	solution composition (wt % malonic acid)							
T (K)	5.6	15.0	28.2	32.0	41.1	47.1	53.0	59.3
274.1	97.4	96.0	93.6	91.9	89.2	88.2	83.6	79.2
277.1	97.5	96.0	93.5	91.8	89.1	88.0	82.8	78.6
281.1	97.5	96.0	93.3	91.8	89.0	87.7	81.9	77.9
285.1	97.6	96.1	93.2	91.8	88.9	87.4	80.9	77.1
289.1	97.6	96.1	93.0	91.8	88.8	87.1	80.0	76.4
293.1	97.7	96.1	92.8	91.8	88.7	86.8	79.1	75.7

(B) Constant Relative Humidity Contours

RH (%)	equation
95	$T = 517.2 - 11.6$(wt %)
90	$T = 553.3 - 7.16$(wt %)
85	$T = -965.3 + 55.8$(wt %) $- [0.616$(wt %)$^2]$
80	$T = 12.85 + 14.74$(wt %) $- [0.1754$(wt %)$^2]$
75	$T = 629.5 - 5.9$(wt %)

(C) Bulk Solution Thermodynamic Equilibrium Lines

equilibrium	equation
ice line	$T = 273.1 - 0.15$(wt %) $- [0.0028$(wt %)$^2]$
S−L coexistence	$T = 151.1 + 2.11$(wt %) $+ [0.0046$(wt %)$^2]$

Oxalic Acid
(D) Relative Humidity

	solution composition (wt % oxalic acid)		
T (K)	7.1	10.7	14.3
283	98.3	b	b
288	96.7	b	b
293	96.7	b	b
298	96.4	97.5	b
303	97.6	96.7	96.2
308	96.9	96.2	95.5
313	97.7	96.8	96.0
318	97.4	97.1	96.6

(E) Constant Relative Humidity Contours

RH (%)	oxalic acid (wt %)
99	4.1
98	8.6
97	13.1

(F) Bulk Solution Thermodynamic Equilibrium Lines

equilibrium	equation
ice line	$T = 273.1 - 0.24$(wt %)
S−L coexistence	$T = 244.5 + 10.92$(wt %) $-$ $[0.796$(wt %)$^2] + [0.0242$(wt %)$^3]$

[a] Shown in Figures 5 and 6 for malonic acid and oxalic acid, respectively. [b] Experiment not done.

bars represent 2 standard deviations. The linear regression (Figure 4, solid line) is used to plot the lines of constant RH in Figure 6 (Table 1E). Also shown in Figure 4 are the results from Peng et al.,[2] and there is good agreement between the two data sets.

3.2. Bulk Solution Measurements: Solid−Liquid Coexistence Curves. Experiments were performed to supplement the data available for the solid−liquid coexistence curves.[22−24] The results for malonic acid and oxalic acid solutions are shown as solid squares in Figure 5 and Figure 6, respectively. The data obtained are in good agreement with literature values, some of which are shown in Figures 5 and 6 as black triangles.[22] There is one anomalous point in the oxalic acid literature, seen in

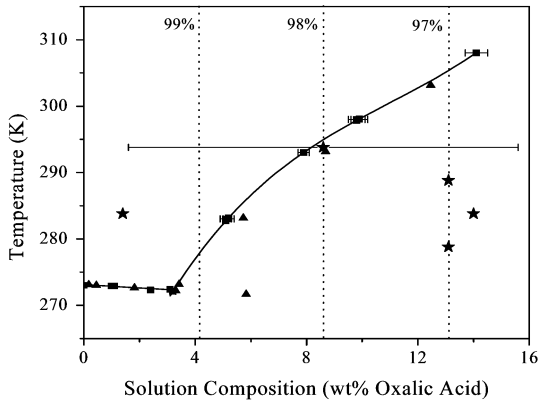

Figure 6. Oxalic acid−H_2O binary phase diagram, with lines of constant RH and experimental results. (—) Ice−$C_2H_2O_{4(aq)}$ (left-hand side) and $C_2H_2O_4 \cdot 2H_2O_{(s)}$–$C_2H_2O_{4(aq)}$ (right-hand side) coexistence curves; (···) constant relative humidity contours; (■) solid−liquid coexistence measurements (error bars represent 2 SD); (▲) literature data.[22] Aerosol experiments: (★) AFT results (error bar representing 1.5% RH is shown to illustrate approximate level of uncertainty in AFT results).

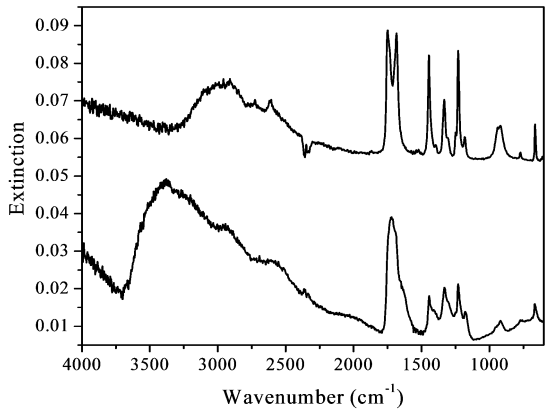

Figure 7. Malonic acid aerosol infrared spectra. (Upper spectrum) Dry malonic acid, RH = 4%; (lower spectrum) aqueous malonic acid aerosol, RH = 95% (gas-phase water lines have been subtracted).

Figure 6 at 5.8 wt %, 271.6 K, that does not fit our experimental data. The solid lines are fits to the data from this study and the known points of the system including the water freezing point (273.15 K), the melting point of the pure dicarboxylic acid, and the eutectic point of the system (260 and 272 K for malonic and oxalic acid, respectively). Fits for these lines are given in Table 1.

3.3. Malonic Acid Aerosol Phase Transitions. Deliquescence-mode experiments for malonic acid particles were performed with both the AFT and the SMC. Deliquescence relative humidities were plotted in Figure 5 by use of the RH contours generated from the vapor pressure experiments. Thus the composition at the deliquescence RH is not measured directly but calculated from the RH data in Table 1. A similar procedure was followed when oxalic acid deliquescence results were plotted in Figure 6. Deliquescence-mode AFT experiments were carried out between 293 and 263 K (Figure 5, ★) and SMC experiments between 277 and 252 K, (Figure 5, ★). Efflorescence-mode experiments were only carried out in the AFT system and were all carried out at 293 or 298 K.

An infrared spectrum of solid malonic acid aerosol is shown in the upper section of Figure 7, and an aqueous malonic acid aerosol spectrum is shown in the lower section. In both, the gas-phase water lines have been subtracted for clarity. The upper spectrum is of aerosol that has passed through the silica dryer

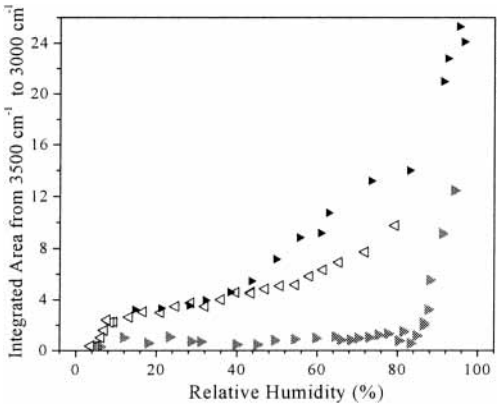

Figure 8. AFT malonic acid aerosol phase transition experiments. The integrated area (3500−3000 cm^{-1}) largely arises from condensed phase water. Two deliquescence mode experiments are shown: The first (gray triangles, 268.9 K), exhibits deliquescence type behavior. The second (solid triangles, 268.9 K), exhibits water uptake. Also shown is an efflorescence mode experiment (open triangles, 293.8 K). Data for the water uptake experiment have been normalized to the C−O mode, ∼1225 cm^{-1} in the 80% RH efflorescence mode spectrum. The integration is performed after subtraction of the lowest RH aerosol spectrum in order to minimize features due to the acid absorption.

and mixed with a flow of 2 L·min^{-1} dry N_2 gas. The solid malonic acid spectrum matches that in the infrared libraries, e.g., Sigma−Aldrich Condensed Phase FTIR Library.[25] Some assigned modes are C−H stretch modes between 3200 and 2500 cm^{-1}, the C═O asymmetric and symmetric stretches at 1749 and 1686 cm^{-1}, the C−OH bend present at 1444 cm^{-1}, and the C−O stretch at 1229 cm^{-1}. Other modes are unassigned.

The aqueous malonic acid spectrum shown in the lower part of Figure 7 is from the same experiment as the dry aerosol spectrum, at a RH higher than the deliquescence RH. There is a characteristic broadening of the modes upon dissolution. The C═O modes become less well resolved and there is a significant decrease in peak intensity for the modes between 1500 and 1100 cm^{-1}. The feature at 920 cm^{-1} almost disappears entirely. In addition, condensed-phase water features are present. Specifically, the OH stretch between 3500 and 2500 cm^{-1} and the hydrogen-bonding mode below 1000 cm^{-1} are readily apparent.

Two modes of behavior were observed in malonic acid deliquescence experiments: (i) water uptake over all relative humidities with no sharp increase in condensed-phase water at the thermodynamic deliquescence RH (black triangles) and (ii) no water uptake until the thermodynamic deliquescence RH (gray triangles). Examples of each type of behavior are shown in Figure 8 along with an efflorescence-mode experiment (open triangles). The residual area of the OH stretch condensed-phase water mode, after subtraction of the lowest RH malonic acid aerosol spectrum, is plotted as a function of RH. The integrated extinction area is over the wavenumber range 3500−3000 cm^{-1}. This area was selected to minimize interferences from gas-phase water lines and the malonic acid C−H modes. In the case of the experiment that exhibited the water uptake, the spectra were normalized to the C−O mode, in the aqueous spectrum at ∼1225 cm^{-1}, at 80% RH from the efflorescence-mode experiment, and the lowest RH spectrum from the efflorescence-mode experiment was used to perform the subtraction. This was in order to correct for the different aerosol populations used in the two experiments and account for the condensed-phase water present in the lowest RH spectrum in the water uptake experiment. The solid spectrum shown in the upper part of Figure 7 is the initial spectrum of an experiment in which the aerosol showed deliquescence behavior, thus supporting the inference that it is

TABLE 2: Summary of Phase Transition Relative Humidities for Malonic Acid and Oxalic Acid: Literature Values and Results from This Work

		malonic acid		oxalic acid		
	T (K)	ERH (%)	DRH (%)	ERH (%)	TRH[a] (%)	DRH (%)
AFT[b]	298.0	6	c	<5		
	293.8	6	69.0		13.5	98
	288.0		80.1		12.7	97
	283.8		80.0		12.6	96.8
	283.8				12.5	99.6
	278.8		79.0		9.0	97
	274.8				14.0	
	273.7		81.1			
	268.7		86.0			
	263.9		83.7			
	263.7				20.0	
	258.7				21.0	
SMC[b]	277.0		82.5			
	276.8		84.8			
	276.6		84.9			
	263.5		85.7			
	260.0		88.3			
	257.7		86.5			
	257.5		87.3			
	252.2		91.2			
Prenni et al.[1]	298	NO[d]	71[e]	NO		99[e]
Peng et al.[2]	298	NO	65.2[f]	51.8−56.7		97.3[f]
Brooks et al.[3]	297		74.3			93
	277		80.6			>95
	263		88.5			
Parsons et al.[26]	295	18.6				
	292		73.7			
	282.9		75.6			
	272.2		80.5			
	263.2		81.7			

[a] Anhydrous to dihydrate phase transition initial RH. [b] This work. [c] Blank spaces indicate the experiment was not done. [d] NO: phase transition not observed. [e] Calculated. [f] Inferred from bulk solutions.

solid malonic acid. Also, the condensed-phase water modes are absent and the modes at <2000 cm^{-1} are sharp and well-resolved.

It became evident that the extent to which the aerosol was dried determined the phase change phenomenon observed. If the aerosol was dried as much as possible (<6% RH), the residual area of the OH stretch remains small and constant with increasing RH until a high RH, where the residual area of the OH stretch increases dramatically, indicating aerosol deliquescence. In this example, the initial RH is 2% and deliquescence occurs at 84%. If insufficient drying occurs in the silica dryer, then a gradual increase in the residual area of the OH stretch is observed over the complete RH range, which implies the aerosol population was not effloresced. The aerosol showing water uptake behavior in Figure 8 was initially at 12% RH. Results from malonic acid experiments over the temperature range 298.0−258.7 K, in which deliquescence was observed, are presented in Table 2.

In the case of the AFT efflorescence experiment shown in Figure 8 (performed at 293 K), the aerosol flow is not passed through the silica dryer and the wet aerosol flow is mixed initially with 2 L·min^{-1} water-saturated N_2. The RH is incrementally decreased and the residual area of the OH stretch is monitored as a function of RH. There is a gradual decrease in the residual area of the OH stretch as relative humidity is decreased, until there is a sharp decrease in area, e.g., at 6% RH in the experiment shown. This decrease in area is concurrent with distinct changes in the subtraction spectrum (not presented here), which supports the interpretation that the phenomenon observed is efflorescence.

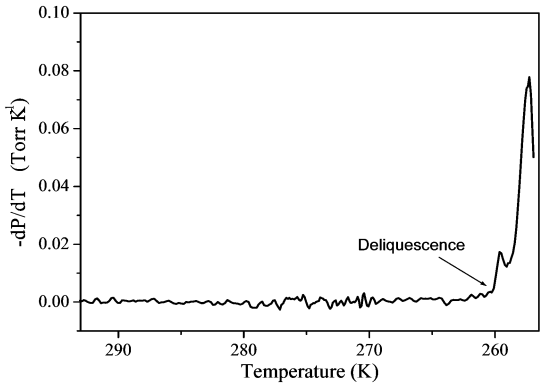

Figure 9. SMC malonic acid aerosol phase transition experiment: $-dP/dT$ as a function of temperature. At deliquescence, water is taken up by the malonic acid particles and the pressure in the chamber decreases.

In addition to AFT experiments, malonic acid particle deliquescence was investigated with the SMC system both above and below the eutectic temperature of the malonic acid−water system (260 K). The SMC results are shown in Figure 5 (★) and summarized in Table 2. As aerosol particles effloresce readily under vacuum conditions, there were no observations of continuous water uptake behavior at relative humidities below the deliquescence point.

During an experiment the pressure in the system (due to water vapor) and the infrared spectrum are monitored as the temperature is lowered. In Figure 9, the rate of change of pressure is plotted as a function of temperature. The pressure is constant ($-dp/dT \sim 0$) until the particles deliquesce and take up water ($-dP/dT > 0$). Concurrent with this change in pressure, the infrared spectrum shifts from that characteristic of a solid to that of an aqueous solution. From the plot of $-dP/dT$ and the temperature at which the IR changes occur, it is possible to calculate the RH at which deliquescence occurs. The second drop in pressure after deliquescence seen in Figure 9 at ~259 K is probably due to heterogeneous freezing.

Within error, the observed deliquescence relative humidities from both the AFT and the SMC experiments follow the equilibrium deliquescence line and its extrapolation below the eutectic temperature of the malonic acid−water system (see Figure 5). This implies that malonic acid behaves in a manner similar to that observed for ammonium sulfate, in that deliquescence occurs below the eutectic temperature leading to the formation of a metastable solution droplet. The lowest temperature at which deliquescence was observable was limited by the ice supersaturation attainable in the chamber. As the DRH of malonic acid is a strong function of temperature, by 250 K the DRH is >90%. Under these conditions in the SMC, ice deposition on the silicon window can occur and DRHs cannot be measured.

3.4. Oxalic Acid Aerosol Phase Transitions. With oxalic acid, two phase transitions were observed: conversion of anhydrous oxalic acid to oxalic acid dihydrate and oxalic acid dihydrate deliquescence to an aqueous solution. Shown in Figure 10 are infrared spectra of the three aerosol phases from an AFT experiment. The gas-phase water subtraction is not as clean as with the malonic acid aerosol spectra. This arises because the low solubility of oxalic acid (11.2 wt % at 297 K)[3] leads to a low absorbance signal due to the acid in the infrared compared to the gas-phase water. In the anhydrous infrared spectrum (Figure 10, upper spectrum) the broad C−H and O−H stretch

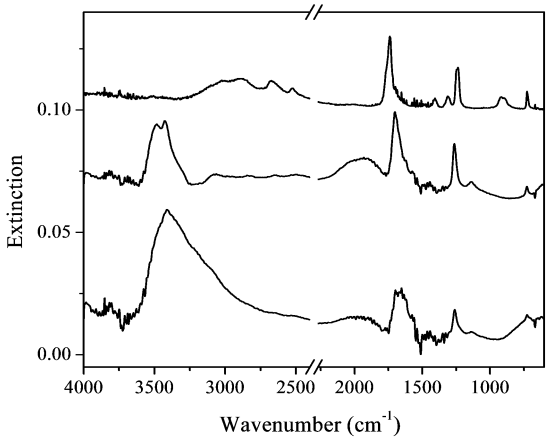

Figure 10. Oxalic acid aerosol infrared spectra. (Upper spectrum) Dry anhydrous oxalic acid, RH = 4%; (center spectrum) oxalic acid dihydrate, RH = 50%; (lower spectrum) aqueous oxalic acid aerosol, RH = 98%. Gas-phase water lines have been subtracted and the spectra have been offset on the *y*-axis. The *x*-axis is split to remove features due to CO_2 impurity.

modes are observed between 3300 and 2500 cm^{-1}. A sharp mode at 1738 cm^{-1} is assigned to C═O and the 1240 cm^{-1} mode to the C−O stretch. Other features in the spectrum have not been assigned. At the transformation to the dihydrate (Figure 10, center spectrum), a strong infrared feature is apparent at 3500−3300 cm^{-1}, the C−H stretch intensity diminishes, a strong feature becomes stronger between 2200 and 1800 cm^{-1}, the C═O shifts to a higher wavenumber, and some of the fine infrared features below 1500 cm^{-1} decrease in intensity or broaden. Both the anhydrous and the dihydrate spectra match the library spectra.[25] In the IR spectrum of deliquesced aerosol (Figure 10, lower spectrum) the condensed-phase water features are present and there is a general broadening of the C═O mode and other oxalic acid features.

As with malonic acid, it was difficult to effloresce oxalic acid aerosol particles. In this case, the aerosol had to be dried to less than 5% RH. This was experimentally difficult due to the lower solubility of the oxalic acid in water; i.e., in order to get to a low RH, more water had to be removed from the aerosol flow by the dryer. When the aerosol was effloresced, no water uptake was observed as RH was increased. If the aerosol was not fully dried, i.e., the aerosol had not effloresced, water uptake over the complete RH range was observed. In the results discussed below, the aerosol was effloresced.

To illustrate the phase transitions as a function of RH, the extinction area 3550−3350 cm^{-1} of the infrared spectrum was integrated after subtraction of the lowest RH spectrum. This area was selected as it is relatively featureless in the anhydrous spectrum, there is a significant feature in the dihydrate spectrum, and the condensed-phase water features grow in upon deliquescence. A sample experiment at 283 K is shown in Figure 11. The phase transition to the dihydrate is observed at RH = 12% ± 2%. At 303 K, anhydrous oxalic acid is predicted to be stable below RH = 11%,[26] above which the oxalic acid dihydrate is the stable phase up to the deliquescence RH. Table 2 summarizes the variation of RH at which the dihydrate transformation is initially observed in the aerosol spectrum as a function of temperature. The phase change RH increases as temperature decreases though the dependence is relatively weak. There are significant changes in the infrared features between the anhydrous and dihydrate phases that were observed to occur until in general about RH = 30%, after which there was no change in the infrared spectrum until deliquescence. This is possibly due to mass transfer limitations for the solid−solid phase transition on the time scale of the experiment in the AFT.

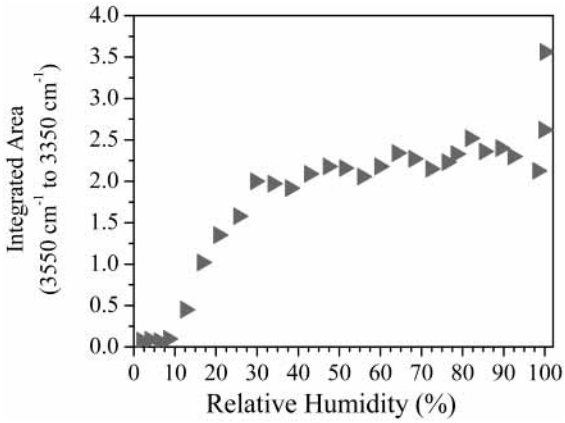

Figure 11. AFT oxalic acid deliquescence mode experiment. Area is integrated after subtraction of the lowest RH spectrum and is due to condensed-phase water.

Deliquescence occurs at RH = 99% for the experiment shown in Figure 11. The DRH results for oxalic acid experiments are plotted on the oxalic acid−water phase diagram in Figure 6. The error bar shown is ±1.5%, which illustrates that within the errors of the experiments deliquescence was observed at the thermodynamically predicted RH. These results, for the temperature range 293−274 K, are summarized in Table 2.

The anhydrous to dihydrate phase transition was observed qualitatively with larger oxalic acid particles/films in the SMC. The phase transition perturbed the water vapor control system; thus only qualitative results were obtained. Nevertheless, the anhydrous oxalic acid to oxalic acid dihydrate phase transition occurred in the SMC after the aerosol had been pumped down to vacuum for several hours. It is thought that the particles are dry under these conditions, and apart from this phase transition, no further changes were observed as the RH was increased. Deliquescence experiments were not performed.

It was only possible with the current AFT experimental apparatus to place an upper limit on the efflorescence RH of oxalic acid. As discussed above, oxalic acid is considerably less soluble than malonic acid. Therefore it was more difficult, with the current experimental flows, to remove sufficient water to get to low enough relative humidities, especially considering that one must initially have aqueous aerosol in efflorescence-mode experiments. At this point we report that the efflorescence occurs at an upper limit of RH = 5% at 293 and 298 K.

4. Discussion and Summary

We have presented experimental data for the solid−liquid coexistence curves, water activity, and aerosol phase transitions for malonic and oxalic acid. We observed that both malonic and oxalic acid aerosols sustain a substantial level of solute supersaturation before particle efflorescence occurs. It is likely that the efflorescence observed in our experiments is homogeneous. We report the deliquescence relative humidities for malonic and oxalic acid aerosols over the temperature ranges 293.8−252.2 and 293.8−278.9 K, respectively. These are among the first published deliquescence relative humidities for these organic acid aerosols. To put our results in context with other recently published data, a summary is presented in Table 2. Prenni et al.[1] characterized the water uptake behavior of dicarboxylic acid aerosols at 298 K using a humidified tandem differential mobility analyzer (HTDMA) and condensation

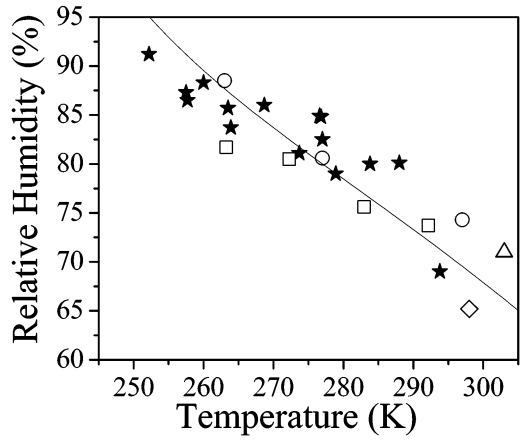

Figure 12. Deliquescence relative humidity as a function of temperature for malonic acid: (★) this work with aerosol; (△) Prenni et al.[1] (calculated); (◇) Peng et al.[2] (bulk); (○) Brooks et al.[3] (bulk); (□) Parsons et al.[27] (aerosol particles); (—) theoretical DRH line from solubility data and literature ΔH_s (see text).

particle counter interfaced with a cloud condensation nuclei counter. Chan and co-workers[2,18,19] have also carried out a series of experiments at 298 K on the "water cycles" of dicarboxylic acids including malonic acid and oxalic acid by use of the electrodynamic balance (EDB) technique both for binary solutions with water and for those with a ternary inorganic component. Very recently Brooks et al.[3] report deliquescence behavior of C_2–C_6 dicarboxylic acid bulk solutions and ternary dicarboxylic acid−ammonium sulfate bulk solution mixtures between 293 and 263 K, and Parsons et al.[27] have used optical microscopy to study particle phase transitions.

In the case of malonic acid, the behavior of aerosol particles in this study is consistent with other studies. We report efflorescence for malonic acid at RH = 6% ± 3% at 298 and 293 K. Malonic acid particles did not effloresce under the experimental conditions of Prenni et al.[1] or Peng et al.,[2] and thus these studies were unable to observe deliquescence. In both of these studies "reversible and continuous water sorption" described particle behavior, consistent with the water uptake curve illustrated in Figure 8. Both studies reported drying the particles to a lowest RH ∼ 5%. This is within error the same RH at which we observed efflorescence, within the error of all the studies. Prenni et al.[1] and Peng et al.[2] may have been just above the ERH for malonic acid. However, Parsons et al.[27] observed a median ERH of 18.6% (range 20.3−16.3%) at 295 K. This value is thought to be an upper limit to homogeneous nucleation because the particles are supported on a surface.

When malonic acid aerosol was dried to a lower RH than that of the ERH, deliquescence was observed at the thermodynamically predicted RH. A comparison of the results from this study with other data (particle, bulk, and calculated) is shown in Figure 12. The inferred value from Peng et al.[2] (DRH = 65.2%), the calculated value from Prenni et al.,[1] (DRH = 71%), the experimental bulk measurements from Brooks et al.,[3] and particle measurements from Parson et al.[27] over the temperature range 292−263 K (see Table 2) are in good agreement with the measurements from the AFT and SMC. The results are in good agreement with the bulk thermodynamic prediction that we have produced by measuring the vapor pressures and equilibrium solid−liquid coexistence curves for malonic acid (shown in Figure 5).

The solid line in Figure 12 is the theoretical variation of DRH with temperature as calculated from the literature heat of solution of malonic acid,[28] $\Delta H_s = 18.8$ kJ·mol^{-1}, and a quadratic fit to malonic acid solubility as a function of temperature, as described in Seinfeld and Pandis.[29] ΔH_s was also calculated both from the data presented in this work and from all the deliquescence RH data shown in Figure 12. These calculations resulted in $\Delta H_s = 12.8$ and 14.7 kJ·mol^{-1}, respectively. Both values are slightly lower than the literature value, though there are significant uncertainties in the calculation that may account for the differences in the literature and calculated values. For oxalic acid, Peng et al.[2] reported an observed ERH of between 51.8% and 56.7%, a region in which we did not observe any phase change in efflorescence-mode experiments. However, they observed some uptake of water at RH > 80% in their deliquescence-mode experiments. This possibly implies that the efflorescence that they observed may not have been full. Alternatively, if there is a strong dependence of the crystallization kinetics on time, the differences may arise from the different time scales of the two experiments or, given that classical nucleation theory predicts the likelihood of a critical embryo being formed is proportional to the volume of the solution and the particles in EDB experiments are much larger than in the aerosol flow tube experiments, the discrepancy may arise from the different volumes of the particles. Prenni et al.[1] did not observe efflorescence down to 5% RH. Here we have reported the first observations of a phase transition of oxalic acid aerosols from the anhydrous to dihydrate form. Our deliquescence results are in agreement with bulk data from Peng et al.[2] and the calculated DRHs presented by Prenni et al.[1] We observe slightly higher DRHs than those of the bulk saturated solutions measured by Brooks et al.[3]

The results from this study lead to preliminary implications for aerosol in the atmosphere. Due to the very high supersaturations achievable by these small dicarboxylic aerosols, should they occur in the condensed phase in the atmosphere it is likely they will be deliquesced and follow the efflorescence/water uptake curves with little hysteresis. However, should the aerosol effloresce heterogeneously, then malonic acid would deliquesce between 69% and 91% RH over the temperature range 293−252.2 K, and for oxalic acid it would require conditions close to 100% RH. One open question is why one observes such a degree of supersaturation. In inorganic systems, which have been comprehensively studied, some salts efflorescence readily (e.g. ammonium sulfate and sodium chloride), whereas others do not, e.g. ammonium bisulfate, ammonium nitrate, and magnesium chloride. The next stage in our work is to consider more chemically complex systems, including the ammoniated dicarboxylic acids and ternary mixtures of dicarboxylic acids with ammonium sulfate.

Acknowledgment. We gratefully acknowledge communication of results from Matt Parsons and Allan Bertram prior to publication and the support from the following institutions: the Natural Sciences and Engineering Research Council of Canada, Canada Foundation for Innovation, Canadian Foundation for Climate and Atmospheric Sciences, and the Ontario Innovation Trust. S.A.S. received support from the Richard Ivey Foundation Summer Research Experience Scholarship.

References and Notes

(1) Prenni, A. J.; DeMott, P. J.; Kreidenweis, S. M.; Sherman, D. E.; Russell, L. M.; Ming, Y. *J. Phys. Chem. A* **2001**, *105*, 11240−11248.

(2) Peng, C.; Chan, M. N.; Chan, C. K. *Environ. Sci. Technol.* **2001**, *35*, 4495−4501.

(3) Brooks, S. D.; Wise, M. E.; Cushing, M.; Tolbert, M. A. *Geophys. Res. Lett.* **2002**, *29*, 1917.

(4) Narukawa, M.; Kawamura, K.; Li, S.-M.; Bottenheim, J. W. *Atmos. Environ.* **2002**, *36*, 2491−2499.

(5) Yao, X.; Fang, M.; Chan, C. K. *Atmos. Environ.* **2002**, *36*, 2099−2109.
(6) Norton, R. B.; Roberts, J. M.; Hueberts, B. J. *Geophys. Res. Lett.* **1983**, *10*, 517−520.
(7) Souza, S. R.; Vasconcellos, P. C.; Carvalho, L. R. F. *Atmos. Environ.* **1999**, *33*, 2563−2574.
(8) Cruz, C. N.; Pandis, S. N. *Atmos. Environ.* **1997**, *31*, 2205−2214.
(9) Cziczo, D. J.; Abbatt, J. P. D. *J. Geophys. Res.* **1999**, *104*, 13781−13790.
(10) Han, J. H.; Martin, S. T. *J. Geophys. Res.* **1999**, *104*, 3543−3553.
(11) Onasch, T. B.; Siefert, R. L.; Brooks, S. D.; Prenni, A. J.; Murray, B.; Wilson, M. A.; Tolbert, M. A. *J. Geophys. Res.* **1999**, *104*, 21317−21326.
(12) Weis, D. D.; Ewing, G. E. *J. Geophys. Res.* **1996**, *101*, 18709−18720.
(13) Koop, T.; Kapilashrami, A.; Molina, L. T.; Molina, M. J. *J. Geophys. Res.* **2000**, *105*, 26393−26402.
(14) Tang, I. N.; Munkelwitz, H. R. *Atmos. Environ. A* **1993**, *27*, 467−473.
(15) Xu, J.; Imre, D.; McGraw, R.; Tang, I. *J. Phys. Chem. B* **1998**, *102*, 7462−7469.
(16) Braban, C. F.; Cziczo, D. J.; Abbatt, J. P. D. *Geophys. Res. Lett.* **2001**, *28*, 3879−3882.
(17) Fortin, T. J.; Tolbert, M. A. *J. Geophys. Res.* **2002**, *107*, article 4088.
(18) Peng, C.; Chan, C. K. *Atmos. Environ.* **2001**, *35*, 1183−1192.
(19) Choi, M. Y.; Chan, C. K. *Environ. Sci. Technol.* **2002**, *36*, 2422−2428.
(20) Cziczo, D. J.; Abbatt, J. P. D. *J. Phys. Chem. A* **2000**, *104*, 2038−2047.
(21) Cziczo, D. J.; Nowak, J. B.; Hu, J. H.; Abbatt, J. P. D. *J. Geophys. Res.* **1997**, *102*, 18843−18850.
(22) Stephen, H.; Stephen, T. *Solubilities of Inorganic and Organic Compounds*, 2nd ed.; Pergamon Press Ltd.: Oxford, 1963; Vol. 1.
(23) Linke, W. F. *Solubilities: Inorganic and metal-organic compounds*, 4th ed.; American Chemical Society: Washington, DC, 1965; Vol. II.
(24) Weast, R. C. *CRC Handbook of Chemistry and Physics*, 68th ed.; Chemical Rubber Co.: Cleveland, OH, 1958.
(25) Sigma−Aldrich. Condensed Phase Infrared Spectra Library; Sigma−Aldrich, Inc., 2002; http://www.sigmaaldrich.com/Technical_Library/Technical_Library_Home.html.
(26) Baxter, G. P.; Lansing, J. E. *J. Am. Chem. Soc.* **1920**, *42*, 419.
(27) Parsons, M. T.; Mak, J.; Lipetz, M. J.; Bertram, A. K. Manuscript in preparation, 2003.
(28) *International Critical Tables of Numerical Data of Physics, Chemistry and Technology*; Washburn, E. W., Ed.; McGraw-Hill Book Company: New York, 1926; Vol. 5, p 148.
(29) Seinfeld, J. H.; Pandis, S. N. *Atmospheric Chemistry and Physics*; John Wiley and Sons Inc.: New York, 1996.